Reprinted from JOURNAL OF APPLIED PHYSICS, Vol. 39, No. 8, 3885–3897, July 1968


# Pressure Dependence of the Plastic Flow Stress of Alkali Halide Single Crystals*

L. A. DAVIS AND R. B. GORDON

*Kline Geology Laboratory, Yale University, New Haven, Connecticut*

(Received 19 February 1968; in final form 25 March 1968)



The change in the plastic yield stress of alkali halide single crystals due to applied hydrostatic pressure has been measured. The pressure dependence of the yield stress ($\delta\sigma/\sigma$) ranges from $\sim 9\times10^{-2}$/kbar in soft RbI to $\sim 0$ in LiF. The experimental results suggest that in soft crystals point-defect generation and/or diffusion is effective in limiting dislocation mobility in the early stages of deformation, whereas in crystals hardened by irradiation or cold work, elastic interactions are rate limiting.

## INTRODUCTION

In order to identify the various activated processes occurring during the plastic deformation of a crystal, measurements of the dependence of the plastic flow stress $\sigma$ on the strain rate, temperature, and pressure are required. Observations of the strain rate and temperature dependence of $\sigma$ are extensive for many materials, but the pressure dependence of $\sigma$ has never been established experimentally. In fact, the early work of Schmid and Boas,[1] which introduced the concept of the critical resolved shear stress, suggests that the normal stress on the slip plane due to hydrostatic pressure should have no effect on $\sigma$; the experiments of Bridgman[2] and of Haasen and Lawson[3] on the plastic flow of metals under pressure reveal little, if any, pressure dependence of $\sigma$. There is such a pressure dependence, however. In the following we report the effect of hydrostatic pressure on $\sigma$ in a number of alkali halide crystals as measured by interrupted compression tests.

## EXPERIMENTS

### Apparatus

Since $\sigma$ is extremely structure sensitive, it is impossible to obtain accurate results from comparisons of compression tests performed at 1 atm with others performed at high pressure. Hence we use the method of interrupted stress–strain ($\sigma$–$\epsilon$) tests on a single specimen. For experiments of this type a testing machine, the minitester, was designed[4] to operate while completely enclosed in a pressure vessel. The results are therefore free of problems of jerky loading and/or load weighing errors which arise if a loading device is brought through a system of high-pressure seals from outside a pressure vessel.

The original minitester has been modified and improved for this series of experiments. The tester, which has a diameter of about 3 cm and is about 38 cm long, consists of a synchronous motor and planetary gear box which turn a 0.3175-cm pitch screw. The rotation of the screw is converted to translation and advances the lower compression platen in the barrel of the tester. The moving platen bears on the sample being tested and the applied force is transferred by a steel rod to a load cell which is, essentially, a very stiff steel spring whose deflection is indicated by strain gauges. The load cell is made from fully hardened Vasco MA steel and contains two thin, parallel arms loaded in tension. Identical strain gauges are mounted on these arms and are connected in series to compensate for bending. The gauges are mechanically bonded to the load cell by the "Rockite" process by the Baldwin–Lima–Hamilton Corporation of Waltham, Massachusetts. For use under high pressure it is necessary that the load-cell material and the strain-gauge bonding material have similar compressibilities.[5] Gauges whose backing is highly compressible, such as epoxy gauges, strip off steel when subjected to a moderate pressure. Experience has shown that Rockite-bonded gauges are reliable through many applications of pressure. The load cells are calibrated at room pressure with an Instron testing machine equipped with an $X$–$Y$ recorder, which allows simultaneous plotting of the applied force and the strain-gauge output of the load cell. The plot of strain vs load for the load cells is approximately linear with a slope of about $1.35\times10^{-6}$/N. Since a strain of $1\times10^{-6}$ is easily detectable, load changes on the order of 0.75 N can be read. As specimens which average 0.6 cm$^2$ in area are generally used, it is possible to detect stress changes of about 0.14 bars.

The driving motor used in the minitester for the compression tests is a hand-wound, single-phase, hysteresis-type, synchronous ac device operating at 25 V and 1800 rpm. When connected through a 60 000:1 gear reducing system to the 0.3175 cm pitch screw, the rate of platen advance in the tester is approximately 0.009 cm/min. As the motor is almost perfectly synchronous, samples are subjected to a

* Research supported by the U.S. Army Research Office, Durham.

[1] E. Schmid and W. Boas, *Plasticity of Crystals* (F. A. Hughes & Co. Ltd., London 1950), p. 103.

[2] P. W. Bridgman, Rev. Mod. Phys. **17**, 3 (1945).

[3] P. Haasen and A. W. Lawson, Z. Metallk. **49**, 6 (1958).

[4] R. B. Gordon and L. F. Mike, Rev. Sci. Instr. **38**, 541 (1967).

[5] R. B. Gordon and J. K. Tien, in *ASME Symposium on High Pressure Technology* (ASME, New York, 1964).

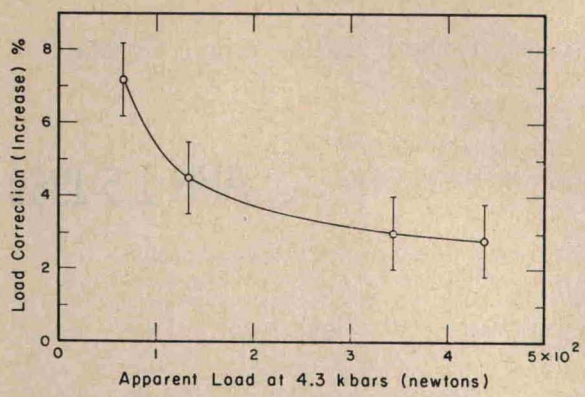


FIG. 1. Pressure dependence of calibration of load cell No. 4 (at 4.3 kbar). The apparent load is computed using the 1-atm calibration.

constant rate of compression. The spring constant for the minitester is about $5\times10^4$ N/cm (comparable to an Instron-type machine). For the highest rate of work hardening observed in the samples tested here the ratio of the plastic compressive deformation rate of the sample to the total deformation rate is $\simeq0.78$. Usually, however, the ratio is in excess of 0.9. Therefore, for the sample length used, 1.8 to 2.54 cm, the plastic compressive strain rate is about $0.5\times10^{-4}$/sec for the rate of platen motion specified above.

In order to compare the flow stresses of a crystal at high and low pressure, it is necessary to determine the effect of pressure on the calibration of the load cell. The procedure adopted for this purpose is to calibrate the load cell *in situ* in the minitester against a helical steel spring both at low and high pressures. Load is generated by compressing the spring against the load cell using the motor-driven platen and the pressure-induced change of calibration is determined by comparing plots of the strain output of the load cell vs time. The applied load, which need not be known explicitly, can be computed knowing the time of loading, the rate of platen advance, the minitester deflection and the spring constant. In comparing plots of load-cell strain vs time, allowance is made for the slight variation of motor speed from test to test ($\sim\pm2\%$) by noting the loading time and the total platen advance at maximum load. This means that the calibration point at the highest load is uniquely determined, but reliability of the points at lower load depends on the constancy of the motor speed with load. Correction for the elastic deflection of the minitester is also made but this is of lesser importance as the tester is rather "hard", i.e., its deflection is small. The load cell used (LC No. 4) is fairly sensitive to pressure, and, in addition, the pressure effect varies with load as shown in Fig. 1. Each point on the figure represents the average of numerous calibration runs. It is believed that the pressure-induced change in calibration is determined to $\pm1\%$, i.e., typically the change in calibration is $4\pm1\%$ at 4.3 kbar for LC No. 4.

The minitester is operated inside a 63.5-cm long, 15.2-cm o.d., 3.17-cm-bore-diam pressure vessel. The vessel is of three-piece construction of a general type described previously.[6] The minitester is placed in the vessel with the motor end down; thus electrical leads brought through the bottom plug connect to the motor and those in the piston connect to the load cell. Pressure is generated by driving the piston with one of two simultaneous acting 500-ton hydraulic rams, while the vessel is advanced by the other ram. Because the effect of even large hydrostatic pressure on the flow stress of the materials studied is moderate, it is not essential to know the applied pressure with great accuracy. Accordingly, the oil pressure in the top 500-ton ram was calibrated against pressure within the vessel by using a 120 Ω manganin gauge whose calibration is based on readings taken with a Harwood DWT-1000 dead-weight tester. Observation of the ram oil pressure allows pressure determination to $\pm0.1$ kbar.

The load-weighing system of an Instron testing machine is used for recording the stress–strain curves (actually, load-cell response vs time) of the samples tested in the minitester. This system allows detection of a force of 0.75 N.

### Materials and Testing Technique

The effect of pressure of 4.3 kbar on the plastic deformation of single-crystal samples of the alkali halides LiF, NaCl, KCl, KBr, KI, RbI, and CsBr was studied. The samples, all of which were purchased from the Harshaw Chemical Co., are in the form of {100} cleavage blocks except in the case of the CsBr which possesses no natural cleavages. CsBr is sawed to shape using a string saw. A great majority of the samples tested were received in the past year but two tests are performed on samples received in 1959 for use in a previous study. The new crystals measure $2.54\times0.64\times0.95$ cm. The older samples are about $1.78\times0.5\times0.5$ cm. The ends of each sample tested are polished flat and parallel by hand using a vee-block. Load is always applied parallel to the largest dimension. The "new" and "old" crystals show a significant difference in flow stress as, due to improved production techniques, the newer crystals are relatively purer and therefore softer. In order to do a controlled study of the effect of crystal strength on the pressure-induced change of flow stress, crystals of different strength were produced by subjecting "new" crystals to 0.1 MR/h $^{60}$Co radiation. The specimens in this case were generally reduced in dimension to $2.54\times0.64\times0.47$ cm in order to lower the applied load necessary to cause yielding. All tests were conducted at room temperature.

The cleavage blocks of the fcc structure alkali halides have four equally stressed primary {110} $\langle\bar{1}10\rangle$ slip systems when loaded in simple compression.

[6] L. A. Davis and R. B. Gordon, J. Chem. Phys. **46**, 2650 (1967).

In the case of LiF, stress birefringence and etch-pit observations show that all four slip systems operate, generally with a definite predominance of slip on one perpendicular set. In NaCl and KCl, stress birefringence observations generally reveal strain on only one mutually perpendicular set of slip planes; the oblique set of slip systems is less likely to operate than in the case of LiF. In CsBr the crystal axis is oriented to within a few degrees of ⟨110⟩ and slip occurs on only one of the possible {110} ⟨001⟩ slip systems.[7] The specimen has {100} and {110} faces.

The interrupted loading technique employed is illustrated schematically in Fig. 2, which shows a plot of stress vs compressive plastic strain. The elastic strain is removed from the recorded traces by measuring from a line drawn parallel to the elastic part of each curve. On the first application of load the plastic strain is anomalously large due to small misalignment of the specimen on the platens but at $A$ a steady state of work hardening is achieved. At $B$ the load on the sample is released. Upon reapplication of the load, the sample starts to flow at a somewhat lower stress as, for example, at $C$. Presumably between $C$ and $D$ dislocations are being pushed back up against barriers from which they have been repelled by long-range interaction forces when the load was released. At $D$, however, a steady state of work hardening is again achieved. The condition that $DE$ is an extension of $AB$, after an arbitrarily long waiting period, is taken to mean that no recovery or aging processes occur while the load is off the sample. In the normal test sequence, then, the load is released at $E$ and the sample is subjected to hydrostatic pressure. On reapplication of the load with the sample now under pressure, the stress–strain curve may look like, for example, that between $E$ and $F$. The high-pressure $\sigma$–$\epsilon$ curve is extrapolated to the fiducial strain

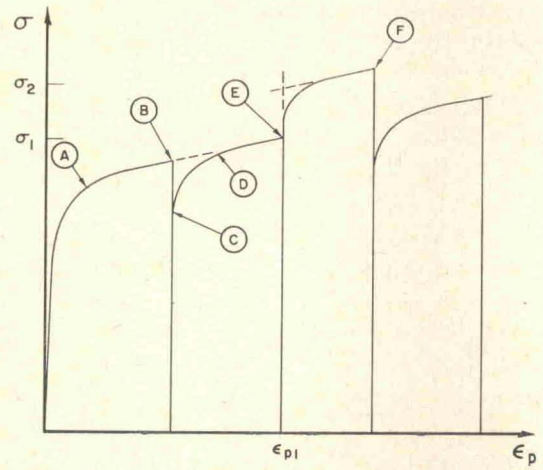


FIG. 2. Schematic stress–strain curve for repeated compression of an alkali halide single crystal. Hydrostatic pressure is applied at $\epsilon_{p1}$.

[7] L. D. Johnson and J. A. Pask, J. Am. Ceram. Soc. **47**, 437 (1964).

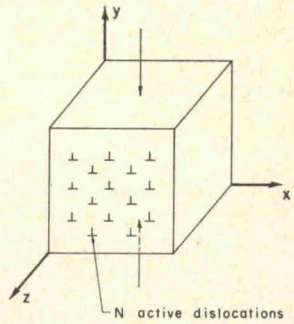


FIG. 3. A single crystal containing $N$ active dislocations to be compressed parallel to the $y$ axis.

as shown; the fractional change in flow stress due to hydrostatic pressure is given by $(\sigma_2-\sigma_1)/\sigma_1=\delta\sigma/\sigma$. At $F$ the load is released, the pressure is released, and on subsequent reapplication of the load at $P=1$ atm there is a change of flow stress of sense opposite to that which occurred when the pressure was applied. In order to study the effect of prestrain, this series of tests can be repeated on a given sample. The entire test procedure is performed with the minitester in the pressure vessel and the sample is thus left undisturbed throughout. It is found that anomalous jumps of flow stress can occur when a sample is moved about on the platens of the minitester.

## INTERPRETATION

In the above described experiment the change in plastic flow stress of a crystal induced by applied hydrostatic pressure is determined. Consider now to which properties of the crystal this flow stress change is related. Imagine a section of a crystal with width $x_1$ and height $y_1$ pierced by $N$ active dislocations all of the same kind, as shown schematically in Fig. 3. Let this crystal be deformed an infinitesimal amount $\Delta y_1$ in time $\Delta t_1$ at $P=1$ atm. The longitudinal strain is given by

$$\Delta\epsilon_1=\phi_1\Lambda_1 b_1\Delta\bar{s}_1, \tag{1}$$

where $\phi_1$ is an orientation factor, $\Lambda_1$ is the dislocation density, $b_1$ is the Burgers vector and $\Delta\bar{s}_1$ is the average distance of dislocation travel. Therefore, for this crystal,

$$\Delta\epsilon_1=\Delta y_1/y_1=\phi_1(N/x_1y_1)b_1\Delta\bar{s}_1. \tag{2}$$

Imagine now the same crystal with the same number of active dislocations to be deformed at elevated pressure an additional infinitesimal amount $\Delta y_1$ in another interval $\Delta t_1$. This is the situation which obtains in the experiment of Fig. 2 where the flow stress change is determined at a single plastic strain and the rate of compression is unaffected by pressure, since the motor speed is effectively the same at 1 atm and 4.3 kbar. Then

$$\Delta\epsilon_2=\Delta y_1/y_2=\phi_2(N/x_2y_2)b_2\Delta\bar{s}_2, \tag{3}$$

where the subscripts 2 indicate quantities at high pressure, i.e., $x_2$ and $y_2$ represent the reduced crystal

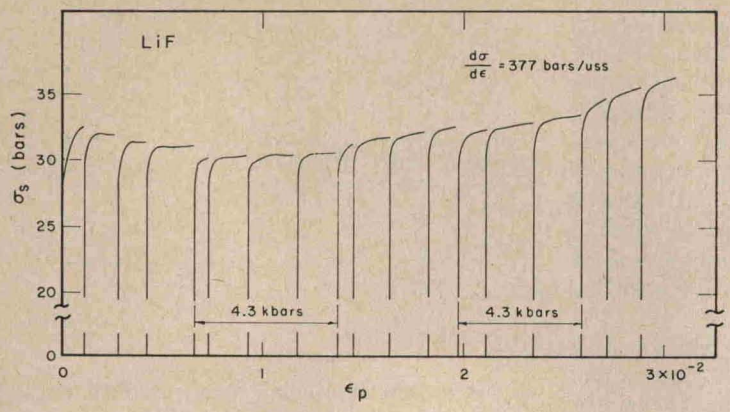


FIG. 4. A shear-stress–shear-strain curve for single-crystal LiF deformed in compression. The 4.3 kbar deformations and the steady-state rate of work hardening (at $\epsilon_p \simeq 3\times10^{-2}$) are noted. Specimen No. 25B.

dimensions at high pressure. For a cubic crystal, the ratio of $b_2$ to $x_2$ equals the ratio of $b_1$ to $x_1$ and $\phi_1$ equals $\phi_2$. Therefore, from Eq. (3),

$$\Delta y_1 = \phi_1 N (b_1/x_1) \Delta\bar{s}_2. \tag{4}$$

From Eqs. (2) and (4) then

$$\Delta y_1/\Delta y_1 = \Delta\bar{s}_2/\Delta\bar{s}_1, \tag{5}$$

so that $\Delta\bar{s}_2 = \Delta\bar{s}_1$ or $\bar{v}_2 = \bar{v}_1$, where $\bar{v}$ is the average dislocation velocity. The change in flow stress with pressure, therefore, is that necessary to maintain a constant dislocation velocity.

It is essential to this argument, of course, that no change in the number of dislocations occur due to application of hydrostatic pressure alone. Etch-pit observations on LiF show that no such change occurs. Also, experiments have been performed where a sample is deformed, then pressurized, without deformation, and redeformed at $P=0$. No discontinuity in flow stress before and after pressurization is found, as would be expected if pressure affected the number of active dislocations. The argument above also assumes that the mode of deformation is identical at elevated pressure and at $P=1$ atm. Etch-pit and stress birefringence observations on LiF, stress birefringence observations on KCl and NaCl, and visual observation of CsBr indicate that this is true.

The condition of constant sample compression rate also depends on the nature of the pressure-induced change in work-hardening rate of a sample. The ratio of the plastic compression rate of a sample to the total deformation rate of the sample and minitester equals $k_m/(k_m+k_s)$, where $k_s$ is the "spring constant" for the plastic compression and $k_m$ is the "spring constant" for the minitester. (The elastic deflection of the sample is negligible in comparison to that of the tester). While $k_m$ is not affected significantly by pressure, it is found that $d\sigma/d\epsilon$ increases under pressure in some cases, increasing $k_s$, and, thus decreasing the plastic compression rate of the sample. This decrease is largest for soft crystals where, for $d\sigma/d\epsilon \simeq 500$ bar/unit shear strain at 1 atm. and $\Delta(d\sigma/d\epsilon)/\Delta P \simeq 50\%$, it amounts to about 6% to 7%. For the harder crystals either the rate of work hardening or the change of rate with pressure or both are smaller so that the effect is negligible. The 6% decrease in plastic compression rate for the soft crystals warrants an addition of $0.4\times10^{-2}$ to $\delta\sigma/\sigma$ to correct to conditions of constant compression rate. However, as the correction is to be made only for the soft crystals, where, it will be seen $\delta\sigma/\sigma$ is large and the experimental scatter is $\sim\pm3$ to $4\times10^{-2}$, the correction is neglected. $\delta\sigma/\sigma$ has of course, been corrected for the change in load-cell calibration with pressure.

## RESULTS

Figure 4 shows a representative interrupted shear stress-plastic shear strain curve ($\sigma_s-\epsilon_p$) for LiF. The sample is one hardened by $^{60}$Co irradiation. Stress and strain are resolved as if they were homogeneous, i.e., $\sigma_s=\sigma_c/2$ and $\epsilon_p=2\epsilon_c$, where the subscript $c$ refers to compression. The results shown in Fig. 4 closely resemble the idealized experiment of Fig. 2; the plastic strain in each cycle is an extension of that in the previous cycle indicating that no recovery or aging has occurred. The change in flow stress due to pressure, $\delta\sigma/\sigma$, is slightly negative, but this falls within the total experimental error. $^{60}$Co irradiation reduces the mobile fraction of dislocations giving rise in some cases (as

TABLE I. Typical work-hardening rate and change of work-hardening rate with pressure.

| | | $W=d\sigma/d\epsilon$ (bar/unit shear strain) | $\sigma_s(\epsilon_p=0)$ (bar) | $d\ln\sigma/d\epsilon$ | $\delta W/W$ ($\delta P=4.3$ kbar) |
|---|---|---|---|---|---|
| LiF | soft | 200 | 10 | 20 | 0 |
| | hard | 500 | 50 | 10 | 0 |
| KI | soft | 340 | 5.2 | 65 | 0.27 |
| KBr | soft | 380 | 5.4 | 70 | 0.21 |
| KCl | soft | 500 | 5.0 | 100 | 0.43 |
| | hard | 290 | 22 | 13 | 0.10 |
| NaCl | soft | 240 | 4.4 | 55 | 0.44 |
| | hard | 120 | 17 | 7 | 0.74 |
| RbI | soft | 400 | 10 | 40 | 0.60 (3.2 kbar) |
| CsBr | soft | 60 | 10 | 6 | 0.34 |
| | hard | 110 | 15.7 | 7 | 0.06 |

shown here) to a yield point not seen in the "as-received" crystals. The broad region of approximately zero work hardening is associated with the expansion of glide bands into undeformed portions of the crystal. When the glide bands fill the crystal, a positive rate of work hardening obtains. It is apparent that the effect of pressure on the flow stress is uninfluenced by whether glide bands do or do not fill the crystal. There is no apparent effect of pressure on the rate of work hardening in either soft, "as-received" crystals or irradiation-hardened crystals (Table I).

The experiment shown in Fig. 4 differs from the ideal of Fig. 2 in that several load cycles are used at each test pressure. This is done so that errors due to "zero-shift" in the load cell (which occur occasionally) will

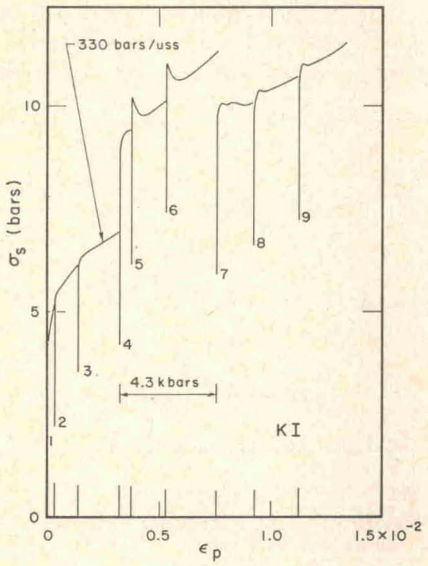


FIG. 5. Shear stress vs shear strain for single-crystal KI (No. 2). The rate of work hardening at 1 atm prior to pressurization is noted.

be detected. Repeated loading sometimes leads to the occurrence (for all of the crystals studied except LiF) of small yield drops in the $\sigma$–$\epsilon$ curve; in successive loading cycles the stress rises slightly higher than the previous maximum stress, before it drops and levels off to the same steady rate of work hardening on a curve extrapolating through the previous work hardening curve. Cycles 5 and 6 in Fig. 5 for soft KI show the most pronounced case of this phenomenon observed; cycles 8 and 9 show a modest, more typical stress increment. This sort of small yield drop has been observed by Haasen and Kelly[8] during interrupted tensile tests on single crystals of pure Ni and Al. They propose that the effect is related to dislocation rearrangements during unloading, rather than to an aging process. For the purposes of extrapolating to the fiducial strain, the steps in the $\sigma_s$–$\epsilon_p$ curve are ignored.

[8] P. Haasen and A. Kelly, Acta Met. **5**, 192 (1957).

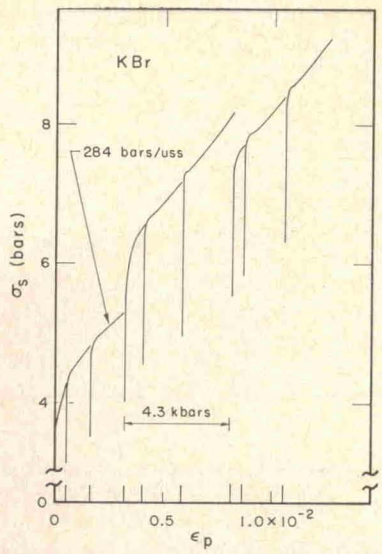


FIG. 6. Shear stress vs shear strain for single-crystal KBr (No. 4A).

In contrast with LiF, KI and KBr show a large increase in flow stress and an increase in work-hardening rate, respectively, under pressure, (Figs. 5 and 6). In both soft (Fig. 7) and irradiated KCl (Fig. 8) a pressure-induced increase in $\sigma_s$ and $d\sigma/d\epsilon$ is evident. Alden[9] has indicated that KCl can show two stages of work hardening with a typical slope in stage I of 180 bar and in stage II of 540 bar. The soft KCl crystals tested deform with only stage-II hardening but KCl crystals

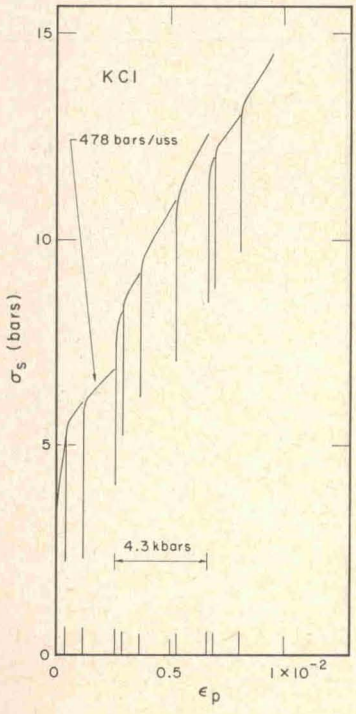


FIG. 7. Shear stress vs shear strain for soft KCl (No. 20).

[9] T. H. Alden, Trans. Met. Soc. AIME **230**, 649 (1964).

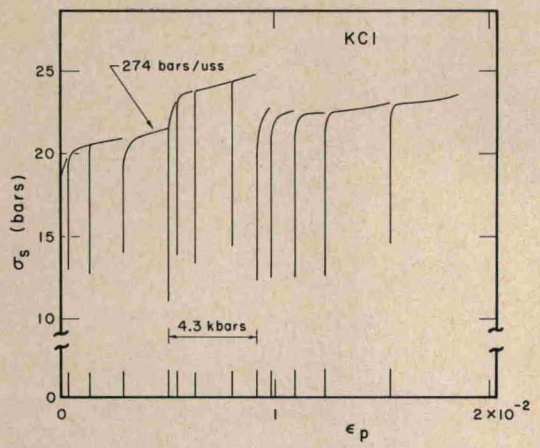


FIG. 8. Shear stress vs shear strain for hard KCl (No. 14A); $d\sigma/d\epsilon$ is less than for soft KCl.

hardened by irradiation exhibit a rate of work hardening more nearly like that of stage I. Another feature observed in Fig. 8 is the occurrance of a region of low work hardening when a crystal is loaded at $P=1$ atm after having been loaded at pressure. This phenomenon occurs on occassion for all the materials tested except LiF and CsBr. It is apparently a work-softening effect analogous to that observed by Stokes and Cottrell[10] for a metal deformed at low temperature and then redeformed at a considerably higher temperature. Stokes and Cottrell found in their experiments that the effect does not arise from the pinning of dislocations by point defects or impurity atoms. They suggest that the dislocation arrangement introduced by low-temperature deformation becomes unstable when deformation at higher temperature is initiated. In the present case the Gilman and Johnston[11] theory of the occurrence of yield points in the alkali halides suggests that the observed pressure-induced work softening may be related to a reduced rate of generation of mobile dislocations in the crystal during plastic deformation at pressure. If the deformation of a crystal from $\epsilon_a$ to $\epsilon_b$ at high pressure generates fewer dislocations than would be generated between $\epsilon_a$ and $\epsilon_b$ by deformation at $P=1$ atm, the occurrence of a yield drop on reinitiation of plastic deformation at $\epsilon_b$ and $P=1$ atm could be expected due to a deficiency in the number of mobile dislocations. A decreased generation rate could occur, for example, if pressure inhibited the occurrence of cross slip. The pressure-induced increase in the work-hardening rate (observed in all the alkali studied except LiF) may be associated with a slower rate of generation

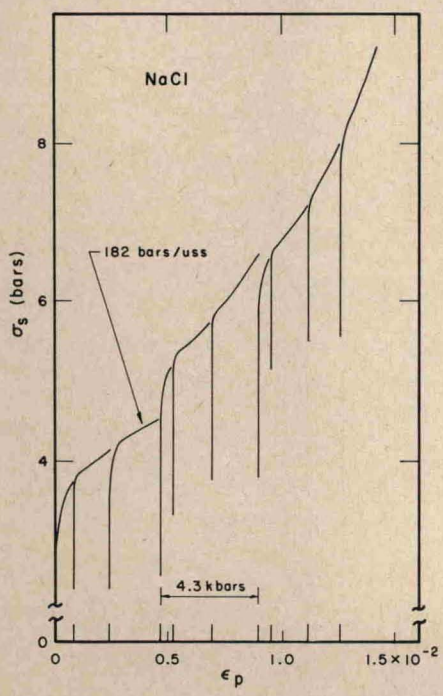


FIG. 9. Shear stress vs shear strain for soft NaCl (No. 27).

[10] R. J. Stokes and A. H. Cottrell, Acta Met. **2**, 343 (1954).

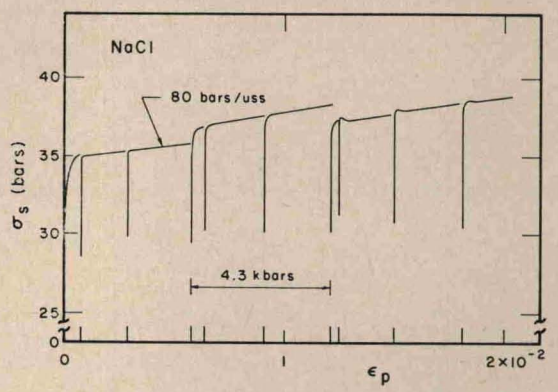


FIG. 10. Shear stress vs shear strain for hard NaCl (No. 26B); $d\sigma/d\epsilon$ is less than for soft NaCl.

of mobile dislocations. When extrapolating the "pressure release" $\sigma_s$–$\epsilon_p$ curve to the fiducial strain it is found that results for $\delta\sigma/\sigma$ consistent with those which occur on pressure application are obtained when the "work-softening" upper yield point is not taken as the flow stress, i.e., the $\sigma$–$\epsilon$ curve is extrapolated below this "yield point."

Figures 9 and 10 give $\sigma_s$–$\epsilon_p$ curves for soft and irradiation hardened NaCl, respectively. The soft NaCl sample of Fig. 9 displays a pressure-induced increase of $\sigma_s$ and $d\sigma/d\epsilon$. In the case of unirradiated crystals there is an occasional tendency for NaCl to show a sudden increase in work-hardening rate, i.e., to enter stage II, under pressure. Comparison of $\sigma$–$\epsilon$ curves for samples deformed at $P=0$ with those for other samples deformed at 4.3 kbar indicates a general tendency for stage I to be shorter at high pressure. Alden found that the rate of stage-I hardening in NaCl is 100–150 bar and the rate of stage II is 400–750 bar. The soft crystals

[11] J. J. Gilman and W. G. Johnston, in *Solid State Physics*, F. Seitz and D. Turnbull, Eds. (Academic Press Inc., New York, 1962), Vol. 13, p. 147.

tested here exhibit an intermediate rate of work hardening. Figure 10, for irradiated NaCl, shows a reduced effect of pressure on $\sigma_s$ compared to soft NaCl; $d\sigma/d\epsilon=$ 80 bar, which is less than for soft NaCl. This indicates, that hardening NaCl by irradiation results in a reduced rate of work hardening.

A $\sigma_s$–$\epsilon_p$ curve for RbI is given in Fig. 11. In this case the applied pressure is only 3.2 kbar as RbI undergoes a phase transition to the CsCl structure at about 3.6 kbar. A large effect of pressure on $\sigma_s$ and $d\sigma/d\epsilon$ is evident. To correct for the change in load-cell calibration at 3.2 kbar it is assumed that the correction shown in Fig. 1 for 4.3 kbar varies linearly with pressure. Figure 12 shows a $\sigma_s$–$\epsilon_p$ curve for CsBr. For the CsBr samples $\sigma_s=0.354\sigma_c$ and $\epsilon_p\cong 2.8\epsilon_c$. Prior to pressure application $d\sigma/d\epsilon=146$ bar and after pressure release it is 60 bar. The $\sigma_s$–$\epsilon_p$ curve has not been shown for high strain but $d\sigma/d\epsilon$ remains approximately constant at 60 bar to much larger $\epsilon_p$. It is concluded that $d\sigma/d\epsilon=60$ bar is the steady-state rate of work hardening at 1 atm and with this as a base $d\sigma/d\epsilon$ is increased by about 35% at 4.3 kbar. Figure 12 indicates that soft CsBr shows a Portevin–Le Chatelier effect (serrated $\sigma_s$–$\epsilon_p$ curve) when deformed under pressure. For soft CsBr the effect is often considerably more pronounced then in Fig. 12; in a crystal hardening by irradiation the oscillations approach 10% of the flow stress.

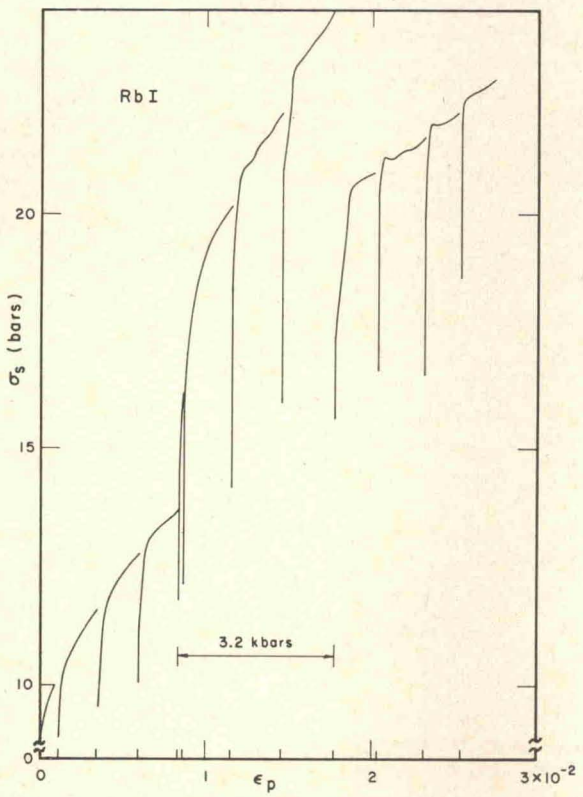


FIG. 11. Shear stress vs shear strain for single-crystal RbI (No. 1); $d\sigma/d\epsilon$ at 1 atm before pressurization is ~400 bar/unit shear strain.

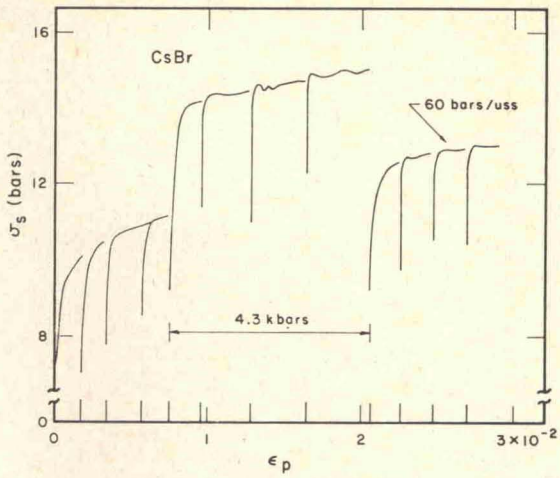


FIG. 12. Shear stress vs shear strain for single-crystal CsBr (No. 1). A serrated $\sigma_s$–$\epsilon_p$ curve is observed at 4.3 kbar.

The $\sigma$–$\epsilon$ curves show the magnitude of $\delta\sigma/\sigma$ to be quite variable even for one specimen. Figure 13 shows all the 4.3 kbar $\delta\sigma/\sigma$ data for KCl plotted vs the low-pressure, shear flow stress resolved in the shear direction. The figure, representing the results obtained on twenty specimens, shows two symbols for each specimen. The open symbol corresponds to the value of $\delta\sigma/\sigma$ on the initial application of pressure. (The open symbol for No. 7 is missing as the initial pressure application was inadvertently made before a steady state of work hardening was achieved.) The shaded symbol is for the value observed on the following release of pressure and for the values on subsequent pressure cycles if they were made. In so far as possible, the shear strain at the points where $\delta\sigma/\sigma$ is measured is kept approximately constant, generally falling in the range of 0.5% to 2% ($\epsilon_s=2\,|\,\Delta l\,|/l_0$). The shear stress of the samples tested ranged from approximately 5 to 40 bar; most high flow-stress values were produced by subjecting samples to $^{60}$Co radiation. It is apparent that $\delta\sigma/\sigma$ falls rapidly in a small range of stress from a maximum value of $25\times10^{-2}$ to a value which remains constant at about $8\times10^{-2}$ to much higher stresses. All the samples which were unirradiated, except Nos. 11, 16, and 23, fall on the nearly vertical part of the curve. The latter samples were work hardened considerably before pressure was first applied and thus show flow stresses intermediate to the softest (as received) and hardest (heavily irradiated) crystals and correspondingly intermediate values of $\delta\sigma/\sigma$. Crystals for which irradiation is lighter show intermediate flow stresses and corresponding $\delta\sigma/\sigma$. It is apparent, therefore, that there is a relationship between shear stress and $\delta\sigma/\sigma$; that is, $\delta\sigma/\sigma$ decreases with $\sigma$ regardless of whether a crystal is hardened by irradiation or work hardening.

A considerable range of $\delta\sigma/\sigma$ exists for the soft crystals. This is probably due in part to slight differences in the crystals, i.e., harder crystals show a

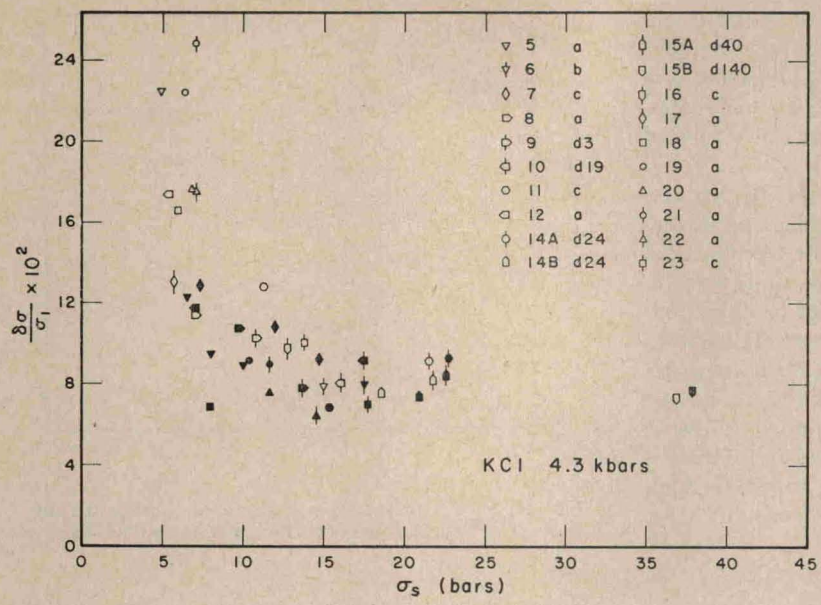


FIG. 13. The 4.3-kbar data for KCl showing the dependence of $\delta\sigma/\sigma$ on shear stress. The data for each specimen are distinguished by a different symbol; unshaded symbols correspond to the first application of pressure and shaded symbols correspond to the release of pressure and to other pressure cycles if they were made. In the legend: $a$=as-received crystal, $b$=as-received 1959 (this crystal is hard mainly due to impurity—it was irradiated for ~0.5 h, however), $c$=work hardened substantially before pressurization, $dx$=$\gamma$-ray irradiated $x$ hours (0.1 MR/h).

smaller effect, and partly because the rate of work hardening in these crystals (relative to the slope of the elastic portion of the stress–strain curve) is very large. The latter phenomenon makes the extrapolation of the high-pressure stress–strain curve to the fiducial strain less reliable. For the harder KCl crystals, or, more generally, for all those experiments where $\delta\sigma/\sigma$ shows little stress dependence, the maximum scatter in $\delta\sigma/\sigma$ is $\pm 2\times 10^{-2}$ about its average at a given stress. The probable error in $\langle\delta\sigma/\sigma\rangle_{\text{av}}$ due to random causes is $\pm 1\times 10^{-2}$. This uncertainty arises from three sources; extrapolation of the $\sigma_s$–$\epsilon_p$ curve to the fiducial strain, load-cell variability, and slight variation in the motor speed from test to test. There is a systematic uncertainty in $\delta\sigma/\sigma$ of $\pm 1\times 10^{-2}$ due to uncertainty in the effect of pressure on the load-cell calibration. The limits of absolute error are, therefore, about $\pm 2\times 10^{-2}$ when $\delta\sigma/\sigma$ has a low stress dependence. We estimate limits of 3 to $4\times 10^{-2}$ for $\delta\sigma/\sigma$ when determined for a soft crystal with rapid work hardening. The variation in $\delta\sigma/\sigma$ with stress in KCl is too large to be accounted for by a combination of random and systematic errors.

Figure 14 shows the dependence of $\delta\sigma/\sigma$ on $\sigma$ in LiF. Within experimental error, $\delta\sigma/\sigma=0$ for this material in all conditions. The $\delta\sigma/\sigma$ vs shear stress data for NaCl are shown in Fig. 15. Over the yield stress range of 5 to 35 bar a decrease in $\delta\sigma/\sigma$ from about $13\times 10^{-2}$ to $\sim 3\times 10^{-2}$ is observed. The experiments on the other alkali halides considered are limited to two each for KI, KBr, and CsBr and one for RbI. As noted above, for the RbI sample $\delta\sigma/\sigma=0.30$ and 0.19 on pressure application and release, respectively. In Fig. 16 $\delta\sigma/\sigma$

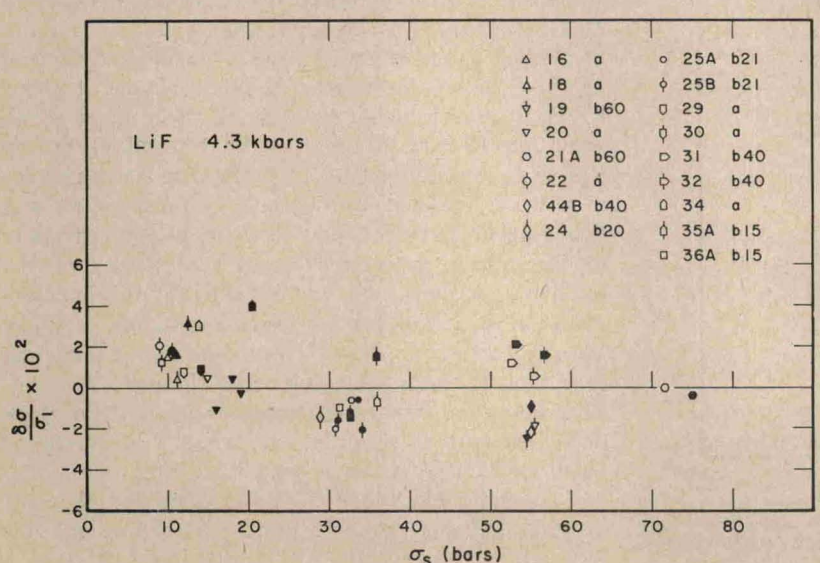


FIG. 14. The 4.3-kbar $\delta\sigma/\sigma$ data for LiF. In the legend: $a$=as received, $bx$=$\gamma$-ray irradiated $x$ min.

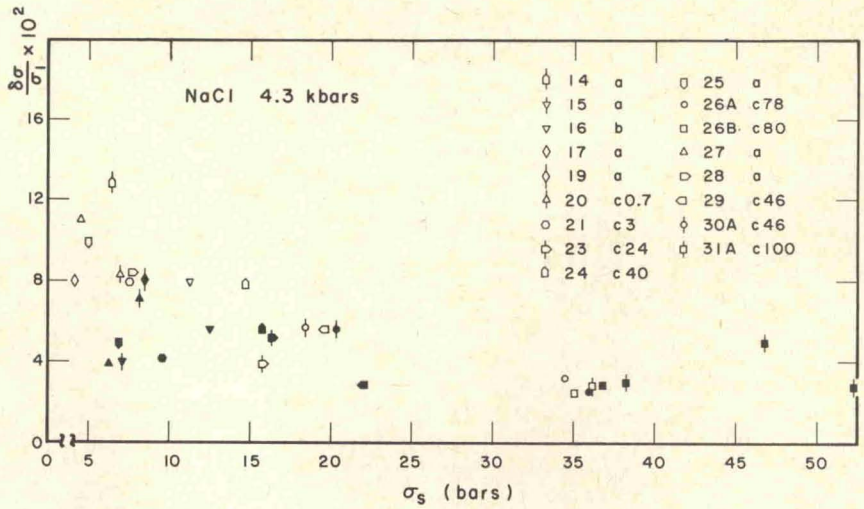


FIG. 15. The 4.3-kbar $\delta\sigma/\sigma$ data for NaCl. In the legend: $a$=as received, $b$=as received 1959 (also irradiated 1 h), $cx$=$\gamma$-ray irradiated $x$ hours.

vs $\sigma_s$ is given for KI, KBr, and CsBr. For KI, $\delta\sigma/\sigma$ varies from a high of 0.33 to a low of ~0.12. The values for KBr range from 0.17 to 0.08. For CsBr $\delta\sigma/\sigma$ shows a maximum of ~0.26 and a minimum of ~0.15. Due to the serrated yielding phenomenon it is impossible to determine $\delta\sigma/\sigma$ on pressure release for the irradiated sample. In each case $\delta\sigma/\sigma$ decreases with $\sigma_s$, although the range of stress covered is not large.

## DISCUSSION

Table II indicates that as one considers the alkali halides in the order of increasing interionic distance, the compression at 4.3 kbar $-\Delta V/V_0$, increases from LiF to RbI and then drops somewhat for CsBr, which has a different structure. As the value of $\delta\sigma/\sigma$, the fractional change in flow stress with pressure, varies in about the same way, to a first approximation there is a qualitative correlation with compressibility. Such a simple correlation offers an inadequate rationalization of the data, however, as the variation of $\delta\sigma/\sigma$ with yield stress indicates. In order to understand the variety of the results, it is necessary to consider in more detail the processes which limit dislocation mobility in a crystal.

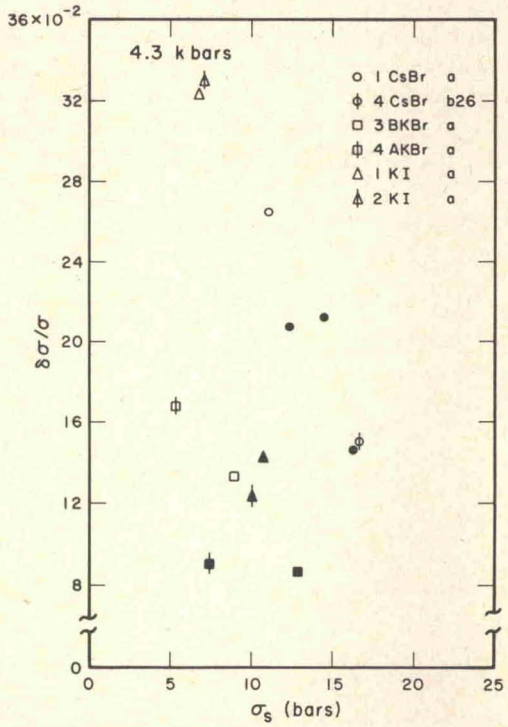


FIG. 16. The 4.3-kbar $\delta\sigma/\sigma$ data for CsBr, KBr, and KI. In the legend: $a$=as received, $bx$=$\gamma$-ray irradiated $x$ hours.

The flow stress of a crystal is the sum of contributions from the Peierls force, $\sigma_P$, the elastic interaction of dislocations with impurity atoms or point defects (isolated or aggregated), $\sigma_E$, the creation of point defects or dragging of pinning points by moving dislocations, $\sigma_{P.D.}$, and dislocation–dislocation elastic interactions, $\sigma_{D-D}$. Due to the sensitivity of flow stress to impurity concentration, it is thought that $\sigma_P$ in the alkali halides is relatively small and that, in the unworked crystal, $\sigma_E$ is the dominant term. Fleischer[12] has analyzed the elastic interaction of randomly dispersed hardening centers with dislocations in cubic materials, distinguishing between "gradual" and "rapid" hardening. Multivalent impurities in the alkali halides produce rapid hardening due to formation of defects of tetragonal symmetry; the increase of $\sigma$ with concentration, $d\sigma/dc$, is $G$ to $10G$, where $G$ is the shear modulus. Fleischer uses isotropic elasticity theory to derive $d\sigma/dc$ in terms of material properties and obtains quantitative results for the rapid increase of flow stress in LiF with irradiation; the tetragonal hardening defect is thought to be an interstitial anion or interstitial cluster. Sibley and Sonder[13] find that the same type of model applies for irradiated KCl.

In Fleischer's analysis, $d\sigma/dc$ is proportional to $G\Delta\epsilon$, where $\Delta\epsilon$ is the tetragonality of the hardening

[12] R. L. Fleischer, Acta Met. **10**, 835 (1962).
[13] W. A. Sibley and E. Sonder, J. Appl. Phys. **34**, 2366 (1963).

TABLE II. Experimental $\delta\sigma/\sigma$ data and calculated variables.

| | $\delta\sigma/\sigma\times10^2$ | $\delta K_s/K_s\times10^2$ | $\delta K_e/K_e\times10^2$ | $-\Delta V/V_0\times10^2$ | $V^*A^3$ | $V_aA^3$ |
|---|---|---|---|---|---|---|
| LiF | 0.4±2 | 2.81 | 3.15 | 0.65 | ~0 | 15.2 |
| NaCl | 13±3 | | | | 21 | 39.0 |
| | 3±2 | 6.33 | 7.21 | 1.84 | 5 | |
| KCl | 25±4 | | | | 38 | 44.7 |
| | 8±2 | 5.83 | 7.21 | 2.47 | 13 | |
| KBr | 17±2 | | | | 28 | 54.6 |
| | ~9 | 7.53 | 9.24 | 3.03 | | |
| KI | 32±3 | | | | 49 | 71.6 |
| | ~13 | 10.3 | 13.0 | 3.90 | | |
| RbI (3.2 kbar) | 30±3 | | | | 63 | 75.3 |
| | ~19 | 6.5 est. | 9.4 est. | 3.09 | | |
| CsBr | 26±2 | | | | 40 | 49.4 |
| | 15±2 | 20.8 | 13.3 | 2.97 | 24 | |

defect. In a material where $\sigma_E$ determines the flow stress, $\delta\sigma/\sigma$ should equal the fractional change of $G$ with pressure, $\delta G/G$, if the degree of tetragonality is unaffected by pressure; $\delta\sigma/\sigma$ should also equal $\delta G/G$ for a heavily work-hardened crystal where $\sigma_{D-D}$ dominates. For anisotropic single crystals, $G$ should be replaced with the appropriate modulus, $K$, for the stress field of a dislocation in an anisotropic material. These moduli have been given by Foreman[14] and are listed with their logarithmic pressure derivatives in Table III for edge and screw dislocations in the NaCl and CsCl structures. The pressure derivatives of the elastic stiffnesses are taken from the compilation by Barsch and Chang.[15] In computing $d\ln K_s/dP$ and $d\ln K_e/dP$, the isothermal elastic moduli and isothermal–isothermal pressure derivatives were used. The values of $dc_{ij}/dP$ given by Barsch and Chang represent the initial slope of the change of modulus with pressure. The assumption is made that $dc_{ij}/dP$ changes linearly with pressure. This is not correct, but most investigations of the pressure dependence of the elastic moduli terminate just when nonlinearity begins. The computed values of $\delta K_s/K_s$ and $\delta K_e/K_e$ for $\delta P=4.3$ kbar (3.2 kbar for RbI) are given in Table II. It is necessary to estimate values for RbI as the required $dc_{ij}/dP$ data are not available. This was accomplished by computing $\delta K_s/K_s$ and $\delta K_e/K_e$ for RbBr at 3.2 kbar and increasing the results in the ratio of the corresponding values for KBr and KI. Table II lists the highest and lowest values of $\delta\sigma/\sigma$ observed for comparison with $\delta K/K$. Figure 17 shows a comparison of $\delta\sigma/\sigma$, $\delta K_e/K_e$ and $\delta K_s/K_s$ for LiF, NaCl, KCl, and

TABLE III. Elastic constants $K$ and their logarithmic derivatives.

NaCl structure

$$K_s=\{[(c_{11}-c_{12})/2]c_{44}\}^{1/2}$$

$$d\ln K_s/dP=\tfrac{1}{2}\{(c_{11}-c_{12})^{-1}d(c_{11}-c_{12})/dP+c_{44}^{-1}dc_{44}/dP\}$$

$$K_e=(c_{11}+c_{12})\{c_{44}(c_{11}-c_{12})/[c_{11}(c_{11}+c_{12}+2c_{44})]\}^{1/2}$$

$$d\ln K_e/dP=K_s^{-1}dK_s/dP-\tfrac{1}{2}\{c_{11}^{-1}dc_{11}/dP+(c_{11}+c_{12}+2c_{44})^{-1}d(c_{11}+c_{12}+2c_{44})/dP\}+(c_{11}+c_{12})^{-1}d(c_{11}+c_{12})/dP.$$

CsCl structure

$$K_s=c_{44}$$

$$d\ln K_s/dP=c_{44}^{-1}dc_{44}/dP$$

$$K_e=(\bar{c}_{12}+c_{12})\{2c_{44}(\bar{c}_{12}-c_{12})/[(c_{11}+c_{12}+2c_{44})\times(\bar{c}_{12}+c_{12}+2c_{44})]\}^{1/2}$$

$$d\ln K_e/dP=(\bar{c}_{12}+c_{12})^{-1}\times d(\bar{c}_{12}+c_{12})/dP+\tfrac{1}{2}\{c_{44}^{-1}dc_{44}/dP+(\bar{c}_{12}-c_{12})^{-1}\times d(\bar{c}_{12}-c_{12})/dP-(c_{11}+c_{12}+2c_{44})^{-1}\times d(c_{11}+c_{12}+2c_{44})/dP-(\bar{c}_{12}+c_{12}+2c_{44})^{-1}\times d(\bar{c}_{12}+c_{12}+2c_{44})/dP\},$$

where $\bar{c}_{12}=\{\frac{1}{2}c_{11}(c_{11}+c_{12}+2c_{44})\}^{1/2}$.

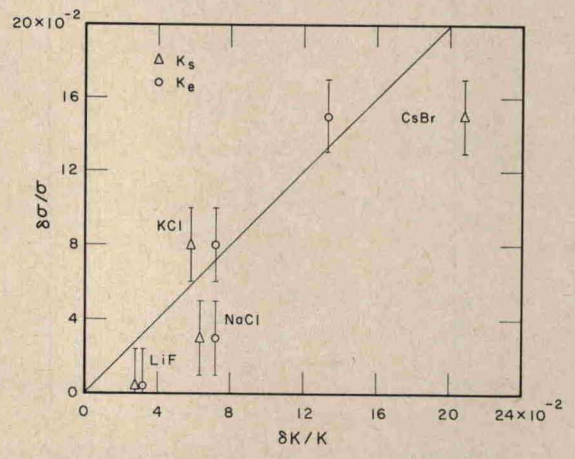


FIG. 17. A comparison of the fractional change of elastic modulus with pressure of 4.3 kbar for edge and screw dislocations with the fractional change of flow stress in hard crystals of LiF, NaCl, KCl, and CsBr.

[14] A. J. E. Foreman, Acta Met. **3**, 322 (1955).

[15] G. R. Barsch and Z. P. Chang, Phys. Status Solidi **19**, 139 (1967).

CsBr. (The properties of hard RbI, KI, and KBr have not been fully investigated.) It is apparent that for LiF, NaCl, and KCl, $\delta\sigma/\sigma$ differs from $\delta K/K_s$ by $3\times10^{-2}$ or less. For LiF and NaCl, $\delta\sigma/\sigma<\delta K_s/K_s$ and for KCl, $\delta\sigma/\sigma>\delta K_s/K_s$. As a consequence, $\delta\sigma/\sigma$ for KCl is more nearly equal to $\delta K_e/K_e$. This suggests that in KCl the mobility of edge dislocations may be more nearly rate limiting while in LiF and NaCl the screws are rate limiting. In fact, the ratio of edge to screw dislocation velocity, $v_e/v_s$, varies from $\sim$50 in LiF[16] to $\sim$10 in NaCl[17] to $\sim$1 to 1.5 in KBr[18] (presumably $v_e/v_s$ is similar in KCl and KBr). For CsBr, we may not have established the lowest possible $\delta\sigma/\sigma$ for hard crystals, but $\delta\sigma/\sigma$ is nearly equal to $\delta K_e/K_e$ suggesting, again, that the mobility of edge dislocations is most important. Although the difference between $\delta\sigma/\sigma$ and $\delta K/K$ (edge or screw) for LiF and NaCl is slightly outside the limits of experimental error, it is clear that the response of flow stress to pressure in hard crystals of LiF, NaCl, KCl, and CsBr could result from the change in elastic interaction between dislocations and defect hardening centers (for irradiated crystals) or other dislocations (for work-hardened crystals). The good agreement between $\delta K/K_{s,e}$ and $\delta\sigma/\sigma$ for the heavily irradiated crystals and the fact that $\delta\sigma/\sigma$ is the same for crystals hardened to a given stress by either irradiation or strain hardening, where defect tetragonality does not enter, suggest that the degree of tetragonality of the hardening defect in the irradiated crystals does not change significantly with pressure.

*Note added in proof:* In the text above, the flow-stress values at high pressure are not corrected for the reduced cross-sectional area of the specimen under pressure. This correction is positive, i.e., $\sigma$ at 4.3 kbar is slightly higher than indicated on the $\sigma$–$\epsilon$ curves, Figs. 4–12, and is given by $(\frac{2}{3})\Delta V/V_0$. The quantity $\Delta V/V_0$ is listed in Table II. This correction increases slightly all the $\delta\sigma/\sigma$ listed in the first column of Table II. For example, $\delta\sigma/\sigma$ for hard LiF corrects to $0.8\times10^{-2}$, for hard NaCl to $4\times10^{-2}$, for hard KCl to $9.6\times10^{-2}$, and for hard CsBr to $17\times10^{-2}$. This creates better agreement between $\delta K_s/K_s$ and $\delta\sigma/\sigma$ for hard LiF and NaCl and places $\delta\sigma/\sigma$ for hard KCl slightly higher above $\delta K_e/K_e$. For CsBr, $\delta\sigma/\sigma$ now falls midway between $\delta K_s/K_s$ and $\delta K_e/K_e$, so that one can no longer suppose which species is rate limiting. For the soft crystals of each type $\delta\sigma/\sigma$ is much larger so the correction is of minor significance. The activation volume $V^*$ (see text) increases only slightly.

The values of $\delta\sigma/\sigma$ observed in soft samples of all the crystals tested except LiF are much too big to be accounted for by an elastic effect, indicating that different mechanisms control plastic flow in the hard and soft crystals. To investigate this, it is useful to consider the activation volume for plastic flow. One can write the relation between mean dislocation velocity $\bar{v}$ and the activation free energy $G^*$ when $\bar{v}$ is determined by a single activated process, as

$$\bar{v}=A\exp(-G^*/kT). \tag{6}$$

The relation can still be used to describe experimental results when more than a single process is active but the derived quantities no longer have simple interpretations in terms of atomic models. The derivative of $\ln\bar{v}$ with pressure, assuming $A$ is insensitive to pressure, is

$$(d\ln\bar{v}/dP)_{T,\sigma}=(d/dP)(-G^*/kT)=-V^*/kT, \tag{7}$$

where $V^*$ is the activation volume (to be distinguished from the quantity having dimensions of volume and given the same name which is obtained from differential strain rate experiments). Equation (7) can be rewritten as

$$V^*/kT=(\partial\ln\bar{v}/\partial\ln\sigma)_{T,P}(\partial\ln\sigma/\partial P)_{T,\bar{v}}, \tag{8a}$$

or, from the strain-rate equation, $\dot{\epsilon}=\Lambda b\bar{v}$, where $\Lambda$ is the mobile dislocation density and $b$ is the Burgers vector, Eq. (8a) can be written as [provided that $(\partial\ln\Lambda/\partial\ln\sigma)_{T,P}=0$]

$$V^*/kT=(\partial\ln\dot{\epsilon}/\partial\ln\sigma)_{T,P}(\partial\ln\sigma/\partial P)_{T,\bar{v}}. \tag{8b}$$

We have determined the second partial derivative in Eq. (8); the first may be obtained directly from strain-rate experiments [Eq. (8b)] or indirectly if one assumes a dislocation velocity–stress model, Eq. (8a). For example, if we choose the model of Gilman and Johnston,[11] $\bar{v}=v_0e^{-D/\sigma}$, where $\sigma$ is the shear stress, $D$, the characteristic drag stress and $v_0$, the shear wave velocity, then $(\partial\ln\bar{v}/\partial\ln\sigma)_{T,P}=D/\sigma$. Equation (8a) can be written then as

$$V^*=(D/\sigma)(kT/\delta P)\ln(\sigma_2/\sigma_1). \tag{9}$$

If a power-law expression is chosen, i.e., $\bar{v}=B\sigma^m$, then $(\partial\ln\bar{v}/\partial\ln\sigma)_{T,P}=m$. Both $D$ and $m$ may be evaluated by dislocation etch-pitting experiments; Nadgornyi and Gutmanas[19] show that such experiments usually yield $m$ in the range 14 to 21 for the alkali halides. The etch-pitting experiments of Johnston and Gilman[16] for LiF give $D/\sigma=18.5$ (for $\sigma$ corresponding to the flow stress). The strain-rate experiments of Phillips[20] give $(\partial\ln\dot{\epsilon}/\partial\ln\sigma)_{T,P}\simeq16$ for both LiF and NaCl, and those of Johnston and Stein[21] yield a value of $\sim$20 at low strain ($\sim$2%) in LiF. Alternatively one can determine $(\partial\ln\bar{v}/\partial\ln\sigma)_{T,P}$ by fitting the strain-rate equation to our 1-atm stress–strain curves. According to the work of Gilman and Johnston[11] and Gilman[22,23] this equation can be written to a good

[16] W. G. Johnston and J. J. Gilman, J. Appl. Phys. **30,** 129 (1959).
[17] É. Y. Gutmanas, É. M. Nadgornyi, and A. V. Stepanov, Sov. Phys.—Solid State **5,** 743 (1963).
[18] V. B. Pariiskii, S. V. Lubenets, and V. I. Startsev, Sov. Phys.—Solid State **8,** 976 (1966).
[19] É. M. Nadgornyi and É. Y. Gutmanas, in *Physical Basis of Yield and Fracture Conference Proceedings* (The Institute of Physics and the Physical Society, London. 1960), p. 266.
[20] W. L. Phillips Jr., Trans. Met. Soc. AIME **224,** 434 (1962).
[21] W. G. Johnston and D. F. Stein, Acta Met. **11,** 317 (1963).
[22] J. J. Gilman, J. Appl. Phys. **36,** 3195 (1965).
[23] J. J. Gilman, J. Appl. Phys. **36,** 2772 (1965).

approximation as

$$\dot{\epsilon}=\phi(\Lambda_0+M\epsilon)bv_0\exp[-(D+W\epsilon)/\sigma], \quad (10)$$

where $\epsilon$ is the shear strain. Here $\Lambda$ is replaced by $(\Lambda_0+M\epsilon)$, where $\Lambda_0$ equals the initial dislocation density and $M\epsilon$ represents the linear increase in dislocation density with strain. (Haasen and Hesse[24] have indicated that a linear dependence does not always hold for the alkali halides, but for moderate strains it should be a fair approximation). The average dislocation velocity, $\bar{v}$, is expressed as $v_0\exp[-(D+W\epsilon)/\sigma]$, where $v_0$ is the limiting dislocation velocity (acoustic velocity of (110) $[\bar{1}10]$ shear waves in the NaCl structure and of (110) [001] shear waves in the CsCl structure) and $(D+W\epsilon)$ is the drag stress of the crystal; $W\epsilon$ represents the change in drag stress with work hardening. Since the strain rate $\dot{\epsilon}$, the Burgers vector $b$, and the appropriate shear-wave velocity $v_0$, are known for the materials tested, only values for $\Lambda_0$ and $M$ need be determined to fit the $\sigma$–$\epsilon$ curves. It would be tedious to determine $\Lambda_0$ and $M$ for every crystal so we have adopted here values of $\Lambda_0$ in the range $10^5$ to $10^6/\text{cm}^2$ (adjusted to achieve the best fit) and $M=10^9/\text{cm}^2$. Gilman[25] indicates that $M=10^9/\text{cm}^2$ is of the correct order of magnitude for LiF and KCl and we assume that it is not greatly different for the other alkali halides. Values of $\Lambda_0$ much less than $10^5$ to $10^6/\text{cm}^2$ lead to very sharp yield drops on initial loading which we do not observe in our crystals. (It is noted that mechanical polishing of the specimens undoubtedly increases $\Lambda_0$ by generating fresh dislocations prior to compression. Some tendencies toward yield-drop formation on initial loading are noted, however, in the heavily irradiated crystals.) Fortunately, $\Lambda_0$ and $M$ enter in a preexponential term so they need only be known approximately. While Eq. (10) itself is only an approximation (in particular, the logarithmic form of the dislocation-velocity–stress relation apparently gives a poor representation of data for soft crystals), it is found to give a reasonably good fit to the $\sigma$–$\epsilon$ curves with the selected values of $\Lambda_0$ and $M$. For the 16 curves fitted for various soft and hard crystals of the alkali halides, $(\partial\ln\bar{v}/\partial\ln\sigma)_{T,P}=(D+W\epsilon)_1/\sigma_1$ (for $\epsilon\sim1\%$) falls between 17 and 21, with an average value near 18.5. [As $v_0\simeq10^5$ cm/sec for all the alkali halides, this indicates, in effect, that the dislocation velocity at the flow stress is $\sim10^{-3}$ cm/sec ($\dot{\epsilon}\simeq10^{-4}$ sec$^{-1}$).] As this value of $(D+W\epsilon)/\sigma$ is in reasonable agreement with the measured values of $m$ and $(\partial\ln\dot{\epsilon}/\partial\ln\sigma)_{T,P}$ given above, we shall use it in Eq. (8) with the appropriate $\delta\sigma/\sigma$, to compute $V^*$.

Figure 13 shows that $\delta\sigma/\sigma$ for soft KCl drops very rapidly in a narrow range of stress. Ideally, if different mechanisms are completely dominant in the hard and soft crystals one would expect to find a constant value of $\delta\sigma/\sigma$ separated by a sharp transition. As no constant value is observed for the soft crystals, it appears that no single rate-limiting mechanism controls plastic flow in the soft material. For the purpose of computing an effective $V^*$ we choose the maximum $\delta\sigma/\sigma$ shown by KCl in Fig. 13 and the maximum $\delta\sigma/\sigma$ shown by the other materials. The values of $\delta\sigma/\sigma$ so chosen and the values of $V^*$ thus computed are listed in Table II. It is apparent that $V^*$ for soft crystals of NaCl, KCl, KBr, KI, and RbI and CsBr is equal to 0.5 to 0.85 of the anion volume $V_a$ which is also shown in the table. (The anion volume is estimated by computing the molecular volume, i.e., the volume of $M^+X^-$, and then assigning portions of this volume to the anion and cation in the ratio of their ionic radii[26] cubed.) This comparison of $V^*$ and $V_a$ suggests that for the soft material the $\sigma_{P.D.}$ term makes an important contribution to the flow stress. A plausible mechanism is vacancy formation by the climb of an edge jog, one ion wide, on a screw dislocation. During climb cation and anion vacancies must be created in succession, but, presumably, the creation of the larger defect is the more difficult step. If this mechanism were rate limiting $V^*$ equal to about $2V_a$ should obtain.[27] That vacancies are generated by plastic deformation is shown by the observed decrease in density of cold-worked KCl.[28] Another possible mechanism is the thermally activated diffusion of impurity pinning points in the stress field of moving dislocations. There are perhaps three possible reasons why, in the present experiments, plastic deformation in the soft crystals is not completely controlled by a "point defect" mechanism. For one, the alkali halides tested, while quite pure,[29] may not be pure enough to eliminate completely the importance of the elastic interaction of impurity atoms and dislocations. In the case of LiF, where $\delta\sigma/\sigma$ is not stress-dependent and the ratio of edge dislocation velocity to screw dislocation velocity is about 50, the jogs or pinning points on screw dislocations may be so firmly anchored that they won't move. Third, in these experiments some work hardening of a crystal occurs prior to determination of $\delta\sigma/\sigma$ (due to $\sim1.0\%$ shear strain), which may give rise to sizable, elastic dislocation–dislocation interactions and/or elastic defect–dislocation interactions, if defects are created by plastic flow. This, in effect, states that the qualitative nature of the mechanism limiting plastic flow in a soft crystal is changed by sufficient work hardening. For example, in Fig. 13 for KCl $\delta\sigma/\sigma$ drops very rapidly with work hardening (increasing $\sigma_s$) in the soft crystals but for the hard crystals, where plastic deformation is pre-

[24] P. Haasen and J. Hesse, Nat. Phys. Lab. G. Brit. Proc. Symp. No. 15, 1, 137 (1963).

[25] J. J. Gilman, Proc. 5th U.S. Nat. Cong. Appl. Mech, (1966).

[26] L. Pauling, *The Nature of the Chemical Bond* (Cornell University Press, Ithaca, N.Y., 1960), p. 526.

[27] D. Lazarus and N. H. Nachtrieb, in *Solids Under Pressure*, W. Paul and D. M. Warschauer, Eds. (McGraw-Hill Book Co., New York, 1963), p. 43–69.

[28] W. H. Vaughan, W. J. Leivo, and R. Smoluchowski, Phys. Rev. 110, 652 (1958).

[29] Crystal purity: LiF, 10–20 ppm total impurity, NaCl<20 ppm, KCl, KBr, KI, CsBr <100 ppm, RbI, unknown. As received condition of the crystals: LiF; grown, annealed (near mp), irradiated, cleaved, and annealed at 400°C for 4 h, all other; grown, annealed (near mp), cleaved.

sumably already governed by the elastic interaction of dislocations and defects and/or other dislocations, $\delta\sigma/\sigma$ shows no dependence on work hardening. It is not unreasonable to expect, then, that in sufficiently pure material the determination of $\delta\sigma/\sigma$ in an etch-pit experiment ($\epsilon_p \simeq 0$) would yield values of $V^*$ considerably larger than found here. Hanafee and Radcliffe[30] have performed etch-pitting experiments on LiF deformed under pressure and find a $V^*$ of about 4 $V_a$ for both soft crystals and hardened, "doped" crystals. They suggest that dislocation motion in LiF is limited (at $\epsilon_p \simeq 0$) by the formation of interstitials by a climbing jog. However, similar experiments on LiF performed at this laboratory[31] give $V^*$ approximately zero for both hard (irradiated) and soft crystals, a result in accord with the compression experiments.

[30] J. E. Hanafee and S. V. Radcliffe, J. Appl. Phys. **38,** 4284 (1967).

## ACKNOWLEDGMENTS

We would like to thank Thomas Blanck for assistance in conducting some of the experiments and Murray Ruggiero for assistance with the high pressure and electronic equipment used, and Professor J. J. Gilman for comments on the interpretation of the results. This research was supported by the U. S. Army Research Office, Durham.

[31] W. L. Haworth, L. A. Davis, and R. B. Gordon, J. Appl. Phys. **39,** 3818 (1968), this issue.